Production of free radicals by the Co^{2+}/Oxone system to carry out diclofenac degradation in aqueous medium

Oscar M. Rodríguez-Narváez, Oracio Serrano-Torres, Kazimierz Wrobel, Enric Brillas and Juan M. Peralta-Hernandez

ABSTRACT

This paper reports the degradation of a solution of 0.314 mM diclofenac (DCF), while using 5–15 mM Oxone as oxidizing agent with the catalytic action of 0.05–0.2 mM Co^{2+}. The best performance was obtained for 10 mM Oxone and 0.2 mM Co^{2+}, achieving the total DCF abatement and 77% removal of chemical oxygen demand after 30 min. Oxidizing of sulfate ($SO_4^{\bullet-}$) and hydroxyl (•OH) radicals was formed by the Co^{2+}/Oxone system. Oxone was firstly oxidized to persulfate ion that was then quickly converted into the above free radicals. For Oxone contents ≥10 mM, the decay of DCF concentration followed a second-order kinetic reaction, but the apparent rate constant changed with the Co^{2+} concentration used. High-performance liquid chromatography (HPLC) analysis of treated solutions showed the formation of some intermediates, whereas oxalic acid was identified as the prevalent final short-linear carboxylic acid by ion-exclusion HPLC.

Key words | Co^{2+}/Oxone system, diclofenac, Fenton-like process, hydroxyl radical, oxidation products, sulfate radical

Oscar M. Rodríguez-Narváez
Oracio Serrano-Torres
Kazimierz Wrobel
Juan M. Peralta-Hernandez (corresponding author)
Departamento de Química, DCNE,
Universidad de Guanajuato,
Cerro de la Venada s/n, Pueblito de Rocha,
Guanajuato, C.P. 36040,
Mexico
E-mail: *juan.peralta@ugto.mx*

Enric Brillas
Laboratori d'Electroquímica dels Materials i del Medi Ambient, Departament de Química Física,
Facultat de Química,
Universitat de Barcelona,
Martí i Franquès 1-11, 08028 Barcelona,
Spain

INTRODUCTION

Recently, an increasing concentration of the so-called emerging pollutants has been detected in natural waters (Rodriguez *et al.* 2017). Drugs are an important group that has been found in the aquatic environment at concentrations from ng L^{-1} to mg L^{-1} (Sirés & Brillas 2012; Pal *et al.* 2014), due to their high recalcitrance and resistance to biodegradation. A ubiquitous drug like diclofenac (DCF) has been detected up to 4.4 μg L^{-1} in surface waters (Moeller *et al.* 2012; Bonnefille *et al.* 2018). DCF ([2-(2,6-dichloroanilino) phenyl]acetic acid, $C_{14}H_{11}NCl_2O_2$), commercialized as Na^+ salt, is a non-steroidal anti-inflammatory drug that can result in human health problems, because the oral consumption of concentrations ≥100 mg can produce gastrointestinal irritations, and superior doses can lead to gastric ulcers (Lagarto *et al.* 2008; Gonzalez-Rey & Bebianno 2014). Moreover, it has been documented that the prolonged exposure to relatively high concentrations of DCF in the environment affects the health of fish, including their renal lesions, alterations of the gills, genotoxicity and estrogenic effects (Gonzalez-Rey & Bebianno 2014). To avoid these problems, the DCF degradation has been the subject of research by conventional water treatments, showing efficiencies close to 90%, but with long retention times (Baccar *et al.* 2012; Melo-Guimarães *et al.* 2013). Advanced oxidation processes (AOPs) have proven their effectiveness for the removal of pharmaceuticals and personal care products from the aqueous phase (Esplugas *et al.* 2007; Miranda-García *et al.* 2010; Bernabeu *et al.* 2011; Sirés & Brillas 2012; Prieto-Rodríguez *et al.* 2013). AOPs are characterized by the generation of hydroxyl radical (•OH), which is a powerful non-selective transient oxidant species that gives rise to the degradation of the most organic pollutants (Rodríguez-Narváez *et al.* 2018). The most ubiquitous AOP is the Fenton's reagent, which involves the catalytic decomposition of hydrogen peroxide using ferrous ion (Fenton reaction) to generate •OH (Yalfani *et al.* 2009). However, the Fenton's reagent possesses several drawbacks like the need for acid pH values for its optimum performance, or the generation of ferric hydroxide sludge that requires an additional separation process and a disposal (Bokare & Choi 2014), which limit its application.

In recent years, to avoid the disadvantages of the Fenton reaction, other oxidant agents (e.g., persulfate or peroxymonosulfate) and transition metals (e.g., cobalt or copper) have

doi: 10.2166/wst.2018.489

been used (Guan *et al.* 2013; Nie *et al.* 2014; Yao *et al.* 2015). These modifications in the Fenton reaction have been called Fenton-like reactions (Wang *et al.* 2016).

A Fenton-like reaction, which showed high efficiency in the removal of organic contaminants, has been the catalytic decomposition of peroxymonosulfate (Oxone, HSO_5^-) with different transition metals (e.g., iron or cobalt) (Wang *et al.* 2016). Oxone decomposition is of great significance mainly because of its capability to be catalytically activated for generating sulfate ($SO_4^{\bullet-}$) and peroxymonosulfate radicals ($SO_5^{\bullet-}$), along with $^{\bullet}OH$ (Anipsitakis & Dionysiou 2003). For many organic pollutants, the oxidation efficiency of the former radical can be even superior to that of $^{\bullet}OH$ (Rodríguez-Narváez *et al.* 2018).

The transition metal which has been found to be the best Oxone catalyst is cobalt (Ghanbari & Moradi 2017). The Co^{2+}/Oxone system has been pre-eminently studied for the application to organics removal, but not for the demonstration of its chemical basis. Several authors have proposed the reactions shown in Equations (1) to (5) involving the production of free radicals ($SO_4^{\bullet-}$ and $^{\bullet}OH$), but their existence has not yet been confirmed experimentally (Anipsitakis & Dionysiou 2003; Chen *et al.* 2007; Shukla *et al.* 2010; Qi *et al.* 2014; Qin *et al.* 2016):

$$HSO_5^- + Co^{2+} \rightarrow Co^{3+} + OH^- + SO_4^{\bullet-} \quad (1)$$

$$HSO_5^- + Co^{3+} \rightarrow Co^{2+} + H^+ + SO_5^{\bullet-} \quad (2)$$

$$2SO_5^{\bullet-} \rightarrow S_2O_8^{2-} + O_2 \quad (3)$$

$$S_2O_8^{2-} + Co^{2+} \rightarrow SO_4^{2-} + SO_4^{\bullet-} + Co^{3+} \quad (4)$$

$$S_2O_8^- + 2OH^- \rightarrow 2SO_4^{2-} + 2\,^{\bullet}OH \quad (5)$$

The aim of this paper is to study the degradation and mineralization of DCF by the Co^{2+}/Oxone system, and the characterization of the $^{\bullet}OH$ radicals produced during the process by Equation (5) to understand the role of generated free radicals. As well, the decay of DCF concentration was analyzed by kinetic models, related to pseudo-first-order and second-order reactions. Oxidation products were detected by the high-performance liquid chromatography (HPLC).

MATERIALS AND METHODS

Reagents

Sodium diclofenac (>99% purity) was purchased from Sigma-Aldrich. Cobalt(II) sulfate heptahydrate and Oxone® ($Oxone + \frac{1}{2}KHSO_4 + \frac{1}{2}K_2SO_4$) were reagent grade purchased from Baker and Sigma-Aldrich, respectively, and used as received. All the solutions were prepared with distilled water. Other chemicals used for analysis were of HPLC or analytical grade purchased from Karal.

DCF degradation

The experiments were performed with 50 mL of a 0.314 mM DCF and 0.1 M phosphate buffer solution in an Erlenmeyer flask at ambient temperature ($24 \pm 2\,^{\circ}C$). An amount of the catalytic Co^{2+} corresponding to 0.05, 0.1 or 0.2 mM was added to the solution, followed by a quantity of the oxidizing agent Oxone corresponding to 5, 10 or 15 mM with vigorous stirring with a magnetic bar to begin the Co^{2+}/Oxone process. The initial pH was 7. Samples of 0.5 mL were withdrawn at the initial time and reaction times of 2, 5, 8, 10, 15, 20, 25, and 30 min to determine the DCF concentration decay by HPLC. To quench the degradation process, 0.5 mL of methanol was added to the reaction mixture immediately after sampling. Trials were made in triplicate and average values are given, along with error bars corresponding to 95% confidence interval in the figures.

Analytical procedures

The DCF concentration was monitored by reversed-phase HPLC using an Agilent Technologies 1200 Series, equipped with a Phenomenex Gemini 5u C-18 (5 μm, 4.6 mm × 150 mm) column at 40 °C and connected to a UV detector set at $\lambda = 280$ nm. The mobile phase consisted of an acetonitrile/methanol/trimethylamine (3 mM, pH 6.2) mixture, which was added with a concentration gradient (Table 1) at a flow rate of 0.8 mL min^{-1}. The peak for DCF appeared at a retention time of 11.4 min.

Generated carboxylic acids were identified and quantified by ion-exclusion HPLC using the above equipment, fitted with a Bio-Rad Aminex HPX 87H (300 mm × 7.8 mm) column at 35 °C and the UV detector selected at $\lambda =$ 210 nm. The mobile phase was 4 mM H_2SO_4 at a flow rate of 0.6 mL min^{-1}.

Table 1 | Concentration gradient table of the mobile phase for the detection of DCF by reversed-phase HPLC

Time (min)	Acetonitrile (%)	Methanol (%)	Triethylamine 3 mM (%)
0	15	15	70
10	45	45	10
11	15	15	70

The chemical oxygen demand (COD) of the samples was directly measured according to the 5220D Standard Method (Clesceri *et al.* 1967). The Oxone concentration was quantified by adding 0.3 mL of concentrated titanium(IV) sulfate to 3 mL of sample and reading the spectrophotometric absorbance at $\lambda = 408$ nm (Eisenberg 1943). The content of Oxone + persulfate was measured following the methodology proposed by Liang *et al.* (2008). An 'A' solution of 0.2 g of $NaHCO_3$ and 4 g KI was prepared in 40 mL of distilled water under stirring, remaining equilibrated after 15 min. A sample of 0.1 mL was added to 40 mL of the 'A' solution and stirred for 10 min, and then its spectrophotometric absorbance was measured at $\lambda = 352$ nm. For the $^{\bullet}OH$ quantification, the procedure of Comninellis (1994) using *N*, *N*-dimethyl *p*-nitrosoaniline (pNDA) was utilized.

RESULTS AND DISCUSSION

Degradation of DCF by the Co^{2+}/Oxone system

Since DCF is only soluble at pH 7, a phosphate buffer was used to follow its degradation (Llinàs *et al.* 2007). Figure 1 depicts the normalized concentration abatement with time for 0.314 mM of DCF using different Oxone concentrations and a Co^{2+} concentration of 0.2 mM. A previous control assay without adding the catalyst can also be observed, showing a 25% DCF decay after 30 min of process. This slow removal is due to the expected oxidation of the amino group of DCF by Oxone (Webb & Seneviratne 1995; Eissen *et al.* 2011). In contrast, Figure 1 highlights a very rapid removal of the drug in the presence of the catalyst up to its total disappearance at 30 min, starting from 10 mM Oxone. The degradation rate increased gradually up to this oxidant agent concentration, but decreased when passing from 10 to 15 mM, indicating that an excess of Oxone caused an inhibition of the process. This behavior agrees with the results reported for the treatment of atrazine with Co^{2+}/Oxone by Ji *et al.* (2015), who concluded that high Oxone content acted as free radical scavenger. To clarify this phenomenon, more trials with different initial contents of Co^{2+} and Oxone were analyzed.

Figure 2 shows the elimination of normalized DCF after the action of 10 and 15 mM Oxone with 0.1 or 0.2 mM Co^{2+}. As can be seen, the increase in the Co^{2+} content always improved the decomposition of the drug with a higher reduction for 10 mM of oxidizing agent with 0.2 mM of Co^{2+}.

The curves of Figures 1 and 2 could be related to a reaction between generated free radicals and DCF according to Equation (6), which gives rise to the second-order kinetic Equation (7) with a second-order rate constant k'_2. Assuming a constant production of free radicals, the pseudo-first-order rate constant k_1 can be defined from Equation (8), and then Equation (7) can be transformed into the pseudo-first-order kinetic Equation (9).

$$\text{Free radicals} + \text{DCF} \rightarrow \text{Products} \tag{6}$$

$$-\frac{d[DCF]}{dt} = k'_2\,[\text{Free radicals}]\,[DCF] \tag{7}$$

$$k_1 = k'_2[\text{Free radicals}] \tag{8}$$

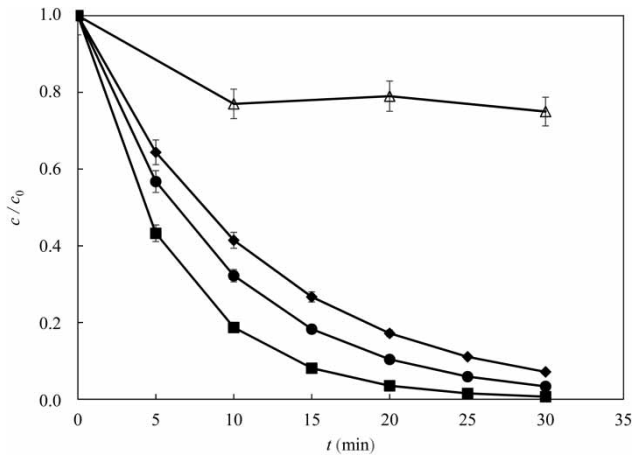

Figure 1 | Normalized DCF degradation ($[DCF]_0 = 0.314$ mM) by the Co^{2+}/Oxone system with 0.2 mM cobalt(II) sulfate and Oxone concentration: (△) 0.0, (◆) 5.0 mM, (■) 10 mM and (●) 15 mM.

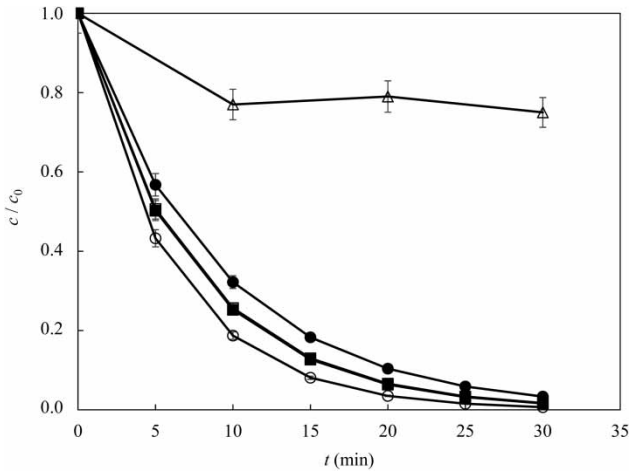

Figure 2 | Normalized DCF degradation ($[DCF]_0 = 0.314$ mM) using the Co^{2+}/Oxone system under the conditions: (●) [Oxone] = 15 mM, $[Co^{2+}] = 0.2$ mM, (■) [Oxone] = 15 mM, $[Co^{2+}] = 0.1$ mM, (○) [Oxone] = 10 mM, $[Co^{2+}] = 0.2$ mM, (□) [Oxone] = 10 mM, $[Co^{2+}] = 0.1$ mM and (△) [Oxone] = 15 mM (control).

Table 2 | Comparison of the pseudo-first-order and second-order rate constants obtained for the removal of 0.314 mM diclofenac with the Co^{2+}/Oxone system under selected conditions

$[Co^{2+}]$ (mM)	[Oxone] (mM)	Co^{2+}/Oxone molar ratio	k_1 (min^{-1})	R^2	k_2 ($mM^{-1}\,min^{-1}$)	R^2
0.2	15	1:75	0.113	0.956	4.90×10^{-4}	0.982
0.1	15	1:150	0.138	0.969	3.91×10^{-3}	0.978
0.05	15	1:300	0.078	0.957	2.88×10^{-3}	0.975
0.2	10	1:50	0.168	0.949	1.31×10^{-2}	0.998
0.1	10	1:100	0.136	0.990	8.47×10^{-3}	0.998
0.05	10	1:200	0.079	0.963	5.21×10^{-3}	0.997
0.2	5	1:25	0.088	0.942	–	–
0.1	5	1:50	0.111	0.955	–	–
0.05	5	1:100	0.089	0.948	–	–

$$-\frac{d[DCF]}{dt} = k_1[DCF] \quad (9)$$

Table 2 summarizes the k_1-values for the Co^{2+}/Oxone concentration ratio and its ability to degrade DCF, along with the corresponding R^2, determined for all the experiments made from the kinetic analysis based on Equation (9). It can be seen that no good R^2-values were obtained for k_1, meaning that Equation (8) is not an appropriate approach to describe the kinetic results, because a non-steady content of free radicals was achieved. Despite this, a comparative discussion of the k_1-values can help to understand the free radical scavenging by Oxone in excess. Thus, for 0.2 mM Co^{2+}, $k_1 = 0.113\ min^{-1}$ was found for 15 mM Oxone, and $k_1 = 0.168\ min^{-1}$, when its concentration was reduced to 10 mM. In contrast, when fewer free radicals were produced using 0.05 mM Co^{2+}, more similar k_1-values close to $0.078\ min^{-1}$ were obtained for 10 and 15 mM of the oxidant agent, although k_1 increased up to $0.089\ min^{-1}$ by reducing oxidant content to 5 mM. These scavenging effects of Co^{2+} can also be observed even for the lower 5 mM of Oxone, since the k_1-value rose from $0.089\ min^{-1}$ for 0.05 mM Co^{2+} to $0.111\ min^{-1}$ for 0.1 mM Co^{2+}, further decaying again to $0.088\ min^{-1}$ for 0.2 mM Co^{2+}. This can be associated with the rise in rate of the parasitic reaction, Equation (10), in which Co^{2+} traps a free radical, such as $SO_4^{\bullet-}$ (Anipsitakis & Dionysiou 2003; Chen *et al.* 2007).

$$Co^{2+} + SO_4^{\bullet-} \rightarrow Co^{3+} + SO_4^{2-} \quad (10)$$

The aforementioned results agree with those reported by other authors who mentioned the importance of Co^{2+} concentration in the Co^{2+}/Oxone system (Ji *et al.* 2015, 2016; Qin *et al.* 2016), but disagree with the assumption of others who presupposed that at great oxidant agent concentration, the highest Co^{2+} content would lead to the highest percentage of degradation, conversely to the trend shown for the k_1-values in Table 2. In this scenario, the kinetic model of Chen *et al.* (2007) confirmed the need for controlling the Co^{2+} concentration, when operating at low quantities of oxidizing agent to avoid the trapping of free radicals.

In Table 2, it is also possible to observe that the Co^{2+}/Oxone ratio presented a phenomenon of inhibition of the DCF oxidation process, if this ratio is greater than 1:200; but for values between 1:50 and 1:150, there is no significant difference in DCF removal ($p = 0.0001$). This is in agreement with the work of Ji *et al.* (2016), where no important changes in tetrabromobisphenol A degradation were observed for molar ratios between 1:120 and 1:160 of Co^{2+}/Oxone.

COD abatement

Figure 3 shows the COD decay determined during 30 min of treatment of 0.314 mM DCF under the best experimental conditions of 10 mM Oxone and 0.2 mM Co^{2+}, as well as for the highest oxidizing agent content of 15 mM Oxone with 0.2 mM Co^{2+}. In the former case, 77% COD removal was found, a value much higher than 48% obtained under the latter conditions. This corroborates that the excess of oxidizing agent allows the consumption of free radicals, which inhibits the degradation process of DCF.

The percentages of COD decay obtained for the DCF solution by the Co^{2+}/Oxone system are consistent with

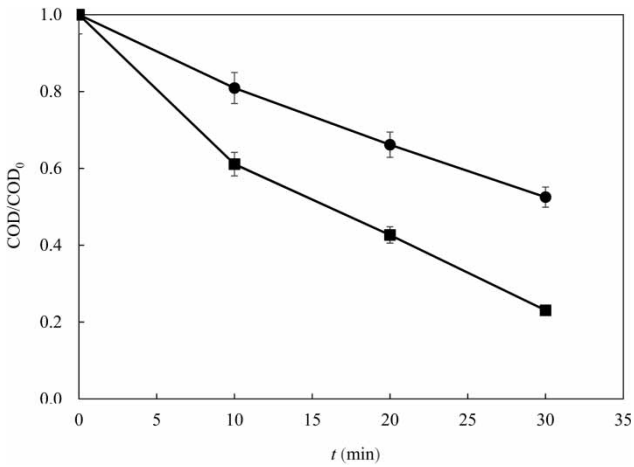

Figure 3 | Normalized COD decay using the Co^{2+}/Oxone system under the conditions: (●) [Oxone] = 15 mM, $[Co^{2+}]$ = 0.2 mM and (■) [Oxone] = 10 mM, $[Co^{2+}]$ = 0.2 mM.

those of Pérez-Estrada *et al.* (2005), who reported a 40.4% COD abatement after 30 min of photo-Fenton treatment of a similar drug solution. Note that such a process involves the generation of high amounts of •OH as free radical, suggesting that in the Co^{2+}/Oxone system, $SO_4^{\bullet-}$ plays a significant role in the DCF removal, apart from •OH.

Identification of oxidation products

As shown in Figure 4(a), the HPLC chromatogram of 0.314 mM DCF displayed a well-defined peak at retention time of 11.4 min. Figure 4(b) evidences that after 30 min of reaction with 10 mM Oxone and 0.2 mM Co^{2+}, the DCF peak was significantly reduced (>98%); in agreement with the data of Figure 2. Moreover, other peaks can be observed at shorter time, which can be related to aromatic products formed from the DCF oxidation process, as well as final carboxylic acids (Pérez-Estrada *et al.* 2005; Michael *et al.* 2014; Mussa *et al.* 2017).

The formation of short-linear aliphatic carboxylic acids during the treatment of 0.314 mM of DCF with 10 mM Oxone and 0.2 mM Co^{2+} was confirmed by ion-exclusion HPLC. From this technique, only one strong adsorption peak at 6.9 min was detected, which was identified as oxalic acid. These results propose that further by-products that are more recalcitrant than carboxylic acids persist in the solution until the end of the electrolysis (Sirés & Brillas 2012). It has also been reported by Pérez-Estrada *et al.* (2005) how the main carboxylic acid was produced under the photo-Fenton treatment of DCF, i.e., when only •OH acted as free radical for its oxidation, as stated above.

Figure 5 highlights a fast generation of oxalic acid during the first 5 min of treatment, then achieves a quasi-steady concentration near 12 mg L^{-1} for longer times, between 10 and 30 min.

This suggests that after an initial quick destruction of the drug yielding a high accumulation of the final oxalic acid, this final by-product is further generated and destroyed practically at the same rate for up to 30 min of treatment, thereby showing a quasi-constant content. These findings evidence the formation of highly persistent by-products to the attack of free radicals ($SO_4^{\bullet-}$ and •OH), even more recalcitrant than oxalic acid, which avoids total DCF mineralization. A mass balance of the final oxalic acid accumulated at 30 min (5.33 mg L^{-1}) indicates that it only contributes 6.22% to the final solution COD of 85.63 mg L^{-1} (Figure 3); therefore, the rest of the COD, as already mentioned above, possibly comes from other recalcitrant products.

Oxone decomposition and second-order kinetics for DCF

Since Oxone is the oxidizing agent used to degrade DCF in the Co^{3+}/Co^{2+} system, blank assays were made to determine the change of Oxone concentration under the above experimental conditions, but without drug addition. As an

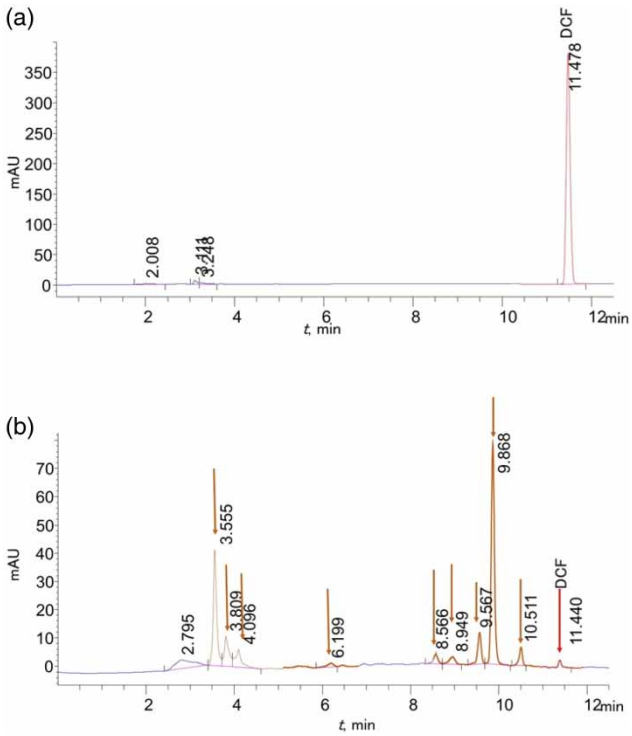

Figure 4 | Reversed-phase HPLC chromatogram for (a) 0.314 mM DCF and (b) after 30 min of reaction of 0.314 mM DCF with 10 mM Oxone and 0.2 mM Co^{2+}.

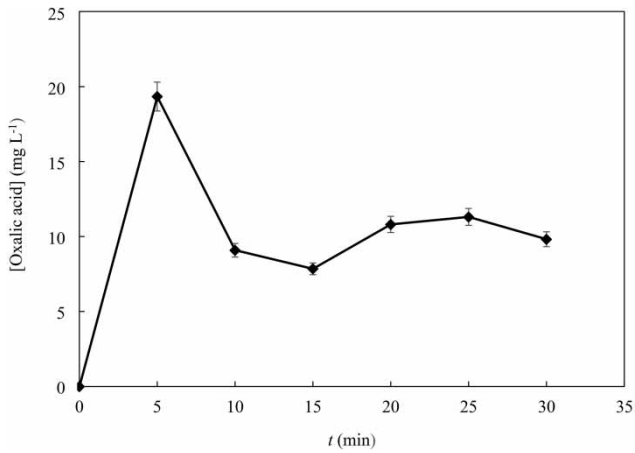

Figure 5 | Time course of oxalic acid concentration detected during the degradation of 0.314 mM DCF by the Co^{2+}/Oxone system with [Oxone] = 10 mM and [Co^{2+}] = 0.2 mM.

example, Figure 6(a) shows the normalized Oxone abatement for a 15 mM solution under the catalytic action of 0.2, 0.1 and 0.05 mM Co^{2+}. As expected, Oxone was more rapidly removed with increasing Co^{2+} concentration due to the acceleration of Equations (1) and (2), and about 95% of it disappeared after 30 min of treatment with 0.2 mM Co^{2+}. Kinetic analysis of the concentration decays showed an excellent agreement with a pseudo-first-order decomposition, since good linear $\ln([Oxone]_0/[Oxone])$ vs. time plots with $R^2 > 0.99$ were found, as can be seen in Figure 6(b).

Once confirmed that the Oxone decomposition fits with a pseudo-first-order kinetic order, it was studied under all experimental conditions, and the results obtained are collected in Table 3. For 15 mM of oxidant agent, an increasing k-value of 0.036, 0.052 and 0.106 min^{-1} was found for 0.05, 0.1 and 0.2 mM Co^{2+}, respectively. However, the rise of the rate constant was not linear, since it only grew

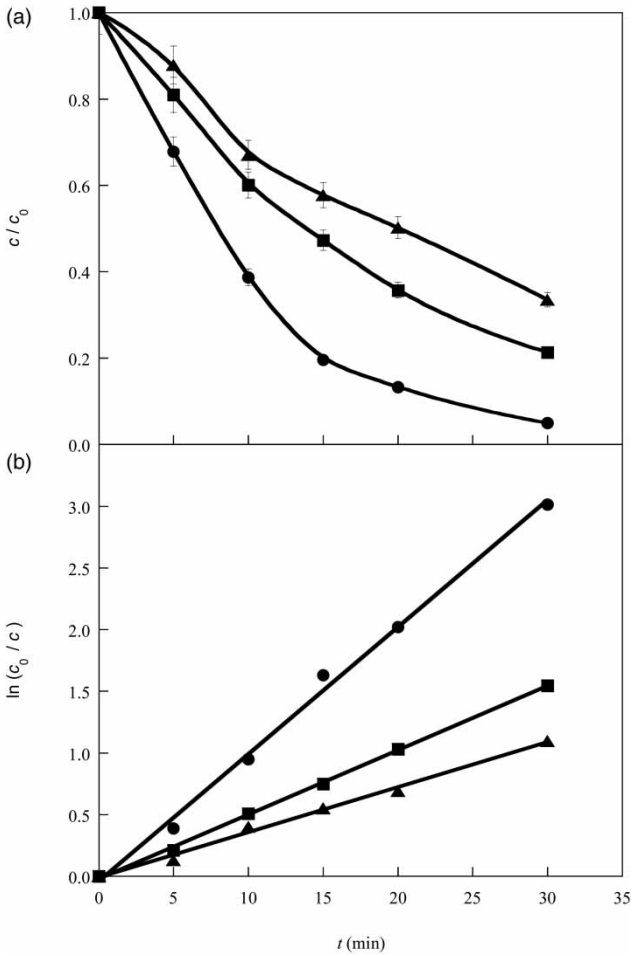

Figure 6 | (a) Normalized Oxone abatement and (b) kinetic analysis considering a pseudo-first order reaction for the removal of 15 mM Oxone by Co^{2+} concentration: (●) 0.2 mM, (■) 0.1 mM and (▲) 0.05 mM.

Table 3 | Comparison of the pseudo-first-order rate constants obtained from Oxone decomposition with Co^{2+} without diclofenac

[Oxone] mM	[Co^{2+}] mM	k min^{-1}	R^2
15	0.2	0.106	0.997
15	0.1	0.052	0.991
15	0.05	0.036	0.998
10	0.2	0.042	0.980
10	0.1	0.054	0.984
10	0.05	0.029	0.976
5	0.2	0.085	0.972
5	0.1	0.733	0.989
5	0.05	0.461	0.981

2.94 times for a fourfold increase of Co^{2+} content. This evidences an increasing loss of the catalytic power of Co^{2+} to oxidize Oxone, because it is more rapidly consumed to destroy the generated $S_2O_8^{2-}$ ion from Equation (4).

When Oxone concentration decreased to 10 mM, the same trend of k as for 15 mM should be expected, but at 10 mM a Co^{2+} excess (0.2 mM) diminished the k-value in comparison with 0.1 mM of Co^{2+} (0.0416 vs. 0.054 min^{-1}). The decrease of k-value with Co^{2+} excess is even more apparent when 5 mM of Oxone was used, because for 0.2 mM it was reduced more than 5 to 10 times, as compared with 0.05 and 0.1 mM, respectively.

Based on the experiments of Oxone decomposition over time given in Table 3, another kinetic model for DCF degradation was tested considering the reaction in Equation (11), where the drug reacts with Oxone, which decomposes to $SO_4^{\bullet-}$ and $^{\bullet}OH$ by Co^{2+} action. This presupposes a second-order reaction rate for two reactants with different initial concentrations, as given by Equation (12).

$$HSO_5^- + DCF \rightarrow \text{Products} \quad (11)$$

$$-\frac{d[DCF]}{dt} = k_2\,[HSO_5^-][DCF] \quad (12)$$

Table 2 shows the k_2-values obtained by this model for 10 and 15 mM Oxone, with good R^2-values between 0.975 and 0.998. As can be seen, for 10 mM Oxone, k_2 rose progressively from 5.21×10^{-3} to 1.31×10^{-2} $mM^{-1}\,min^{-1}$, when Co^{2+} grew from 0.05 to 0.2 M. This means that it is not a true rate constant, and its increasing value informs about the expected greater production of free radicals ($SO_4^{\bullet-}$ and $^{\bullet}OH$) at higher catalyst content. In the case of 15 mM Oxone, Table 2 evidences a maximum

$k_2 = 3.91 \times 10^{-3}$ mM^{-1} min^{-1} for 0.1 mM Co^{2+}, decreasing for the highest 0.2 mM concentration. This behavior, along with the lower k_2-values found for 15 mM and compared to 10 mM Oxone under all conditions and the information of Table 3, suggests that Oxone decomposes with the cobalt, but when it is in excess, not all the oxidants generated could attack the DCF, since some of them could produce $SO_5^{\bullet-}$ from Equation (13) (Ghanbari & Moradi 2017), which possessed much lower oxidation potential.

$$HSO_5^- + SO_4^{\bullet-} \rightarrow SO_4^{2-} + SO_5^{\bullet-} + H^+ \quad (13)$$

The lack of k_2-values in Table 2 for 5 mM of oxidizing agent is also noticeable; it was so rapidly and completely destroyed that it gave rise to inconsistent negative rate constants. This allows the conclusion that the second-order kinetic model seems valid for Oxone concentrations $\geq$10 mM and a molar ratio of Co^{2+}/Oxone < 1:300. However, the limitations and discrepancies of this model indicate that the k_1-values of the pseudo-first-order model describe more appropriately the behavior of DCF decay.

Persulfate and hydroxyl radical evolution

To clarify the oxidation power of the Co^{2+}/Oxone process, the evolution of the generated persulfate ion was assessed following the spectrophotometric method of Liang *et al.* (2008). It was expected that this oxidant was formed from the combination of two $SO_5^{\bullet-}$ anion radicals by Equation (3), and consequently, its evolution profiles could inform about the relative proportion of Co^{2+} and Co^{3+} that affected the rates of Equations (1)–(5), especially for the production of the oxidizing free radicals $SO_4^{\bullet-}$ and •OH, originating from their destruction by Equations (4) and (5), respectively. Tests were made with a 15 mM Oxone solution upon addition of 0.05, 0.1 and 0.2 mM Co^{2+}. Surprisingly, no $S_2O_8^{2-}$ was accumulated in the two former solutions, whereas decreasing concentrations of 1.809 and 0.760 mM of this ion were detected at 1 and 2 min of the latter process, respectively. The presence of accumulated persulfate under these conditions can be associated with a very rapid initial oxidation of Oxone via Equations (1)–(3) by the high 0.2 mM Co^{2+} content in the solution. Nevertheless, the subsequent quicker removal of persulfate by Equations (4) and (5) could account for its complete disappearance at longer time, as well as when less Oxone concentration is present in the reaction medium.

The above results evidence the quick activation of persulfate by Co^{2+}. Several authors have also described the use of persulfate with transition metals to degrade organics (Liang & Guo 2010; Qi *et al.* 2014; Wu *et al.* 2017). In a comparative study of Liang & Guo (2010) on the treatment of naphthalene with persulfate catalyzed with Co^{2+} and zero-valent iron, a much faster activation of persulfate was found with the former ion.

Finally, several assays were made with pNDA solutions containing 10 and 15 mM Oxone and 0.2 or 0.1 mM Co^{2+} to determine the ability of Co^{2+}/Oxone to generate •OH. For the low pNDA concentrations (<1 mM), maximum •OH production was found at 1 min of treatment, but its low content limited a detailed assessment of further evolution. Better results were obtained for 15 mM pNDA solution, i.e., the same concentration as for the oxidizing agent. Figure 7(a) highlights the evolution of accumulated •OH found for these trials. For 0.2 mM Co^{2+}, a very rapid accumulation of this radical up to 5.30 mM occurred during the first 2.5 min of treatment, whereupon its production stopped to achieve a content near 7.3 mM at 10 min. In contrast, this phenomenon was not observed for 0.1 mM Co^{2+}, where •OH was continuously produced

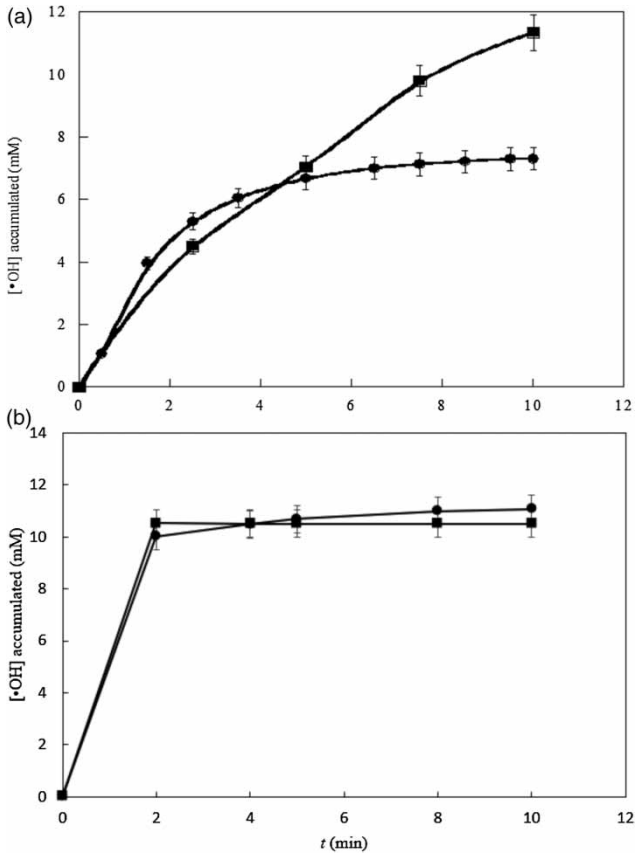

Figure 7 | Concentration of hydroxyl radical accumulated in (a) 15 mM and (b) 10 mM Oxone and Co^{2+} concentration: (●) 0.2 mM and (■) 0.1 mM.

up to 11.3 mM. However, when Oxone concentration was reduced at 10 mM (Figure 7(b)), a very fast •OH content (almost 11 mM) was produced in a similar way for both Co^{2+} concentrations during the first 2 min of reaction.

The high amount of •OH generated, when compared to Oxone decomposition concentration, could be related to the different reactions proposed to produce •OH in the Co^{2+}/Oxone system from Equations (5), (14) and (15) by Ghanbari & Moradi (2017):

$$HSO_5^- + H_2O \rightarrow SO_4^{2-} + 2\,^{\bullet}OH + H^+ \quad (14)$$

$$SO_5^{\bullet-} + 2H_2O \rightarrow SO_4^{2-} + 3\,^{\bullet}OH + H^+ \quad (15)$$

Our results then evidence that the relative proportion of generated $SO_4^{\bullet-}$ and •OH depends on the Co^{2+} content, tested at the given Oxone concentration, the formation of the former oxidant being more favorable than the latter for 15 mM Oxone by using higher amounts of catalyst. This fact can explain the superior oxidation ability of 0.1 over 0.2 mM Co^{2+} to degrade DCF under these conditions (see Figure 2) because of the greater production of the more potent oxidant •OH, associated with the higher k_1- and k_2-values obtained for 0.1 mM Co^{2+} (see Table 2). However, this phenomenon was not observed for 10 mM Oxone, where both rate constants increased progressively at greater catalytic amount (see Table 2), because •OH was more largely produced (Figure 7(b)) than $SO_4^{\bullet-}$ in all cases.

Note that Nie *et al.* (2014) suggested that at acid pH, the predominant free radical from the thermal activation of persulfate is $SO_4^{\bullet-}$, compared to •OH. Our results confirm the same behavior for 15 mM Oxone and 0.2 mM Co^{2+} at long treatment time, whereas at the beginning of the process, •OH is largely produced. The much smaller production of the latter radical by means of other AOPs is also noticeable (Aurioles-López *et al.* 2016; Huesca-Espitia *et al.* 2017; Luis Sánchez-Salas *et al.* 2017; Ramírez-Sánchez *et al.* 2017). For instance, Huesca-Espitia *et al.* (2017) reported a maximum •OH concentration of 0.05 mM after 50 min of Fenton reaction with a Fe^{2+}/H_2O_2 molar ratio of 1:30. The Co^{2+}/Oxone system tested possessed stronger oxidation ability, since it was able to produce near 220-fold higher •OH concentration using 15 mM Oxone and 0.1 mM Co^{2+} (see Figure 7).

CONCLUSIONS

The Co^{2+}/Oxone system achieved the degradation of a DCF solution with an efficiency >95% in a span of 30 min, with 77% of COD removal. The excess of Oxone caused a scavenging effect over the oxidizing free radicals formed. The proportion of $SO_4^{\bullet-}$ and •OH depended on the Co^{2+} and Oxone concentrations, being more favorable the formation of the former oxidant for higher contents of both reactants. Persulfate ion, generated from Oxone oxidation, was not accumulated in the reaction medium, because it was rapidly transformed into the above free radicals. From the Oxone decay, it was found that the DCF abatement obeyed the second-order kinetics for Oxone concentrations $\geq$ 10 mM, but the apparent rate constant varied with the amount of Co^{2+} used, owing to the different relative proportion of both free radicals formed under each experimental condition. Oxalic acid, originating from the cleavage of the benzene moiety of aromatic intermediates, was identified as the final by-product by ion-exclusion HPLC.

ACKNOWLEDGEMENTS

The authors would like to acknowledge the economic support from the Universidad de Guanajuato under the Project No. 18 (Convocatoria Institucional de Apoyo a la Investigación Científica 2018). O. M. Rodriguez-Narvaez also would like to thank CONACyT for the graduate fellowship and la Universidad Autónoma de Nayarit for the scholarship as well. O. M. Rodriguez-Narvaez would also like to thank CONACyT for the graduate fellowship and the provided facilities of Mass Spectrometry Laboratory, under the Project CONACyT grant LN 294024.

REFERENCES

Anipsitakis, G. P. & Dionysiou, D. D. 2003 Degradation of organic contaminants in water with sulfate radicals generated by the conjunction of peroxymonosulfate with cobalt. *Environmental Science & Technology* **37** (20), 4790–4797.

Aurioles-López, V., Polo-López, M. I., Fernández-Ibañez, P., López-Malo, A. & Bandala, E. R. 2016 Effect of iron salt counter ion in dose-response curves for inactivation of *Fusarium solani* in water through solar driven Fenton-like processes. *Physics and Chemistry of the Earth* **91**, 46–52. https://www.sciencedirect.com/science/article/pii/S1474706515001254 (accessed 7 November 2017).

Baccar, R., Sarr, M., Bouzid, J., Feki, M. & Blanquez, P. 2012 Removal of pharmaceutical compounds by activated carbon prepared from agricultural by-product. *Chemical Engineering Journal* **211–212**, 310–317. http://dx.doi.org/10.1016/j.cej.2012.09.099.

Bernabeu, A., Vercher, R. F., Santos-Juanes, L., Simón, P. J., Lardín, C., Martínez, M. A., Vicente, J. A., González, R., Llosá, C., Arques, A. & Amat, A. M. 2011 Solar photocatalysis as a tertiary treatment to remove emerging pollutants from wastewater treatment plant effluents. *Catalysis Today* **161** (1), 235–240.

Bokare, A. D. & Choi, W. 2014 Review of iron-free Fenton-like systems for activating H_2O_2 in advanced oxidation processes. *Journal of Hazardous Materials* **275**, 121–135.

Bonnefille, B., Gomez, E., Courant, F., Escande, A. & Fenet, H. 2018 Diclofenac in the marine environment: a review of its occurrence and effects. *Marine Pollution Bulletin* **131**, 496–506. https://www.sciencedirect.com/science/article/pii/S0025326X18302844 (accessed 11 October 2018).

Chen, X., Qiao, X., Wang, D., Lin, J. & Chen, J. 2007 Kinetics of oxidative decolorization and mineralization of Acid Orange 7 by dark and photoassisted Co^{2+}-catalyzed peroxymonosulfate system. *Chemosphere* **67** (4), 802–808.

Clesceri, L., Greenberg, A. E. & Eaton, A. D. 1967 Standard methods for the examination of water and wastewater. *Health Laboratory Science* **4**, 137–141. http://www.ncbi.nlm.nih.gov/pubmed/17489283.

Comninellis, C. 1994 Electrocatalysis in the electrochemical conversion/combustion of organic pollutants. *Electrochimica Acta* **39** (1), 1857–1862.

Eisenberg, G. M. 1943 Colorimetric determination of hydrogen peroxide. *Industrial & Engineering Chemistry Analytical Edition* **15** (5), 327–328.

Eissen, M., Strudthoff, M., Backhaus, S., Eismann, C., Oetken, G., Kaling, S. & Lenoir, D. 2011 Oxidation numbers, oxidants, and redox reactions: variants of the electrophilic bromination of alkenes and variants of the application of oxone. *Journal of Chemical Education* **88** (3), 284–291.

Esplugas, S., Bila, D. M., Krause, L. G. T. & Dezotti, M. 2007 Ozonation and advanced oxidation technologies to remove endocrine disrupting chemicals (EDCs) and pharmaceuticals and personal care products (PPCPs) in water effluents. *Journal of Hazardous Materials* **149** (3), 631–642.

Ghanbari, F. & Moradi, M. 2017 Application of peroxymonosulfate and its activation methods for degradation of environmental organic pollutants: review. *Chemical Engineering Journal* **310**, 41–62. http://dx.doi.org/10.1016/j.cej.2016.10.064.

Gonzalez-Rey, M. & Bebianno, M. J. 2014 Effects of non-steroidal anti-inflammatory drug (NSAID) diclofenac exposure in mussel *Mytilus galloprovincialis*. *Aquatic Toxicology* **148**, 818–831. https://www.sciencedirect.com/science/article/pii/S0166445X14000150 (accessed 11 October 2018).

Guan, Y. H., Ma, J., Ren, Y. M., Liu, Y. L., Xiao, J. Y., Lin, L. q. & Zhang, C. 2013 Efficient degradation of atrazine by magnetic porous copper ferrite catalyzed peroxymonosulfate oxidation via the formation of hydroxyl and sulfate radicals. *Water Research* **47** (14), 5431–5438. https://www.sciencedirect.com/science/article/pii/S0043135413005149 (accessed 7 November 2017).

Huesca-Espitia, L. L. d. C., Aurioles-López, V., Ramírez, I., Sánchez-Salas, J. L. & Bandala, E. R. 2017 Photocatalytic inactivation of highly resistant microorganisms in water: a kinetic approach. *Journal of Photochemistry and Photobiology A: Chemistry* **337**, 132–139. http://dx.doi.org/10.1016/j.jphotochem.2017.01.025.

Ji, Y., Dong, C., Kong, D. & Lu, J. 2015 New insights into atrazine degradation by cobalt catalyzed peroxymonosulfate oxidation: kinetics, reaction products and transformation mechanisms. *Journal of Hazardous Materials* **285**, 491–500.

Ji, Y., Kong, D., Lu, J., Jin, H., Kang, F., Yin, X. & Zhou, Q. 2016 Cobalt catalyzed peroxymonosulfate oxidation of tetrabromobisphenol A: kinetics, reaction pathways, and formation of brominated by-products. *Journal of Hazardous Materials* **313**, 229–237.

Lagarto, A., Bueno, V., Martínez, A., García, R., Lara, M., Fernández, A., Gabilondo, T., Valdés, O., Carrillo, C. & Montero, C. 2008 Irritación gástrica producida por diclofenaco de sodio : estudio comparativo de tabletas de liberación controlada en conejos. *Revista de Toxicología* **25** (1–3), 32–37. http://www.redalyc.org/html/919/91925305/ (accessed 24 January 2018).

Liang, C. & Guo, Y. Y. 2010 Mass transfer and chemical oxidation of naphthalene particles with zerovalent iron activated persulfate. *Environmental Science and Technology* **44** (21), 8203–8208.

Liang, C., Huang, C. F., Mohanty, N. & Kurakalva, R. M. 2008 A rapid spectrophotometric determination of persulfate anion in ISCO. *Chemosphere* **73** (9), 1540–1543.

Llinàs, A., Burley, J. C., Box, K. J., Glen, R. C. & Goodman, J. M. 2007 Diclofenac solubility: independent determination of the intrinsic solubility of three crystal forms. *Journal of Medicinal Chemistry* **50** (5), 979–983.

Sánchez-Salas, J. L., Aguilar Ubeda, A., Gómez, B. F., Máynez Navarro, O. D., Méndez Rojas, M. A., Reyna Tellez, S. & Bandala, E. R. 2017 Inactivation of bacterial spores and vegetative bacterial cells by interaction with ZnO-Fe_2O_3 nanoparticles and UV radiation. *AIMS Geosciences* **3** (4), 498–513. http://www.aimspress.com/article/10.3934/geosci.2017.3.498.

Melo-Guimarães, A., Torner-Morales, F. J., Durán-Álvarez, J. C. & Jiménez-Cisneros, B. E. 2013 Removal and fate of emerging contaminants combining biological, flocculation and membrane treatments. *Water Science and Technology* **67** (4), 877–885.

Michael, I., Achilleos, A., Lambropoulou, D., Torrens, V. O., Pérez, S., Petrović, M., Barceló, D. & Fatta-Kassinos, D. 2014 Proposed transformation pathway and evolution profile of diclofenac and ibuprofen transformation products during (sono)photocatalysis. *Applied Catalysis B: Environmental* **147**, 1015–1027. https://www.sciencedirect.com/science/article/pii/S0926337313006607 (accessed 11 October 2018).

Miranda-García, N., Maldonado, M. I., Coronado, J. M. & Malato, S. 2010 Degradation study of 15 emerging contaminants at low concentration by immobilized TiO_2 in a pilot plant. *Catalysis Today* **151** (1–2), 107–113.

Moeller, G. B., Gerardo, P. & Drogui, P. 2012 Problemática, importancia y orientación de los contaminantes emergentes en agua potable y aguas residuales. In: *Contaminantes Emergentes: su Importancia, Retos y Prespectivas Sobre la Medición, el Tratamiento y su Reglamento* (G. Moeller & G. Buelna, eds).

Instituto Mexicano de Tecnología del Agua, Mexico City, Mexico, p. 149.

Mussa, Z. H., Al-Qaim, F. F., Othman, M. R., Abdullah, M. P., Latip, J. & Zakria, Z. 2017 Pseudo first order kinetics and proposed transformation products pathway for the degradation of diclofenac using graphite–PVC composite as anode. *Journal of the Taiwan Institute of Chemical Engineers* **72**, 37–44. https://www.sciencedirect.com/science/article/pii/S1876107016305417 (accessed 11 October 2018).

Nie, M., Yang, Y., Zhang, Z., Yan, C., Wang, X., Li, H. & Dong, W. 2014 Degradation of chloramphenicol by thermally activated persulfate in aqueous solution. *Chemical Engineering Journal* **246**, 373–382. http://dx.doi.org/10.1016/j.cej.2014.02.047.

Pal, A., He, Y., Jekel, M., Reinhard, M. & Gin, K. Y. H. 2014 Emerging contaminants of public health significance as water quality indicator compounds in the urban water cycle. *Environment International* **71**, 46–62. http://dx.doi.org/10.1016/j.envint.2014.05.025.

Pérez-Estrada, L. A., Malato, S., Gernjak, W., Agüera, A., Thurman, E. M., Ferrer, I. & Fernández-Alba, A. R. 2005 Photo-Fenton degradation of diclofenac: identification of main intermediates and degradation pathway. *Environmental Science and Technology* **39** (21), 8300–8306.

Prieto-Rodríguez, L., Oller, I., Klamerth, N., Agüera, A., Rodríguez, E. M. & Malato, S. 2013 Application of solar AOPs and ozonation for elimination of micropollutants in municipal wastewater treatment plant effluents. *Water Research* **47** (4), 1521–1528.

Qi, C., Liu, X., Lin, C., Zhang, X., Ma, J., Tan, H. & Ye, W. 2014 Degradation of sulfamethoxazole by microwave-activated persulfate: kinetics, mechanism and acute toxicity. *Chemical Engineering Journal* **249**, 6–14.

Qin, W., Fang, G., Wang, Y., Wu, T., Zhu, C. & Zhou, D. 2016 Efficient transformation of DDT by peroxymonosulfate activated with cobalt in aqueous systems: kinetics, products, and reactive species identification. *Chemosphere* **148**, 68–76. http://dx.doi.org/10.1016/j.chemosphere.2016.01.020.

Ramírez-Sánchez, I. M., Tuberty, S., Hambourger, M. & Bandala, E. R. 2017 Resource efficiency analysis for photocatalytic degradation and mineralization of estriol using TiO_2 nanoparticles. *Chemosphere* **184**, 1270–1285.

Rodriguez, O., Peralta-Hernandez, J. M., Goonetilleke, A. & Bandala, E. R. 2017 Treatment technologies for emerging contaminants in water: a review. *Chemical Engineering Journal* **323**, 361–380. http://linkinghub.elsevier.com/retrieve/pii/S1385894717306502.

Rodríguez-Narváez, O. M., Pérez, L. S., Yee, N. G., Peralta-Hernández, J. M. & Bandala, E. R. 2018 Comparison between Fenton and Fenton-like reactions for L-proline degradation. *International Journal of Environmental Science and Technology* 5–8. http://link.springer.com/10.1007/s13762-018-1764-1 (accessed 25 May 2018).

Shukla, P., Wang, S., Singh, K., Ang, H. M. & Tadé, M. O. 2010 Cobalt exchanged zeolites for heterogeneous catalytic oxidation of phenol in the presence of peroxymonosulphate. *Applied Catalysis B: Environmental* **99** (1–2), 163–169.

Sirés, I. & Brillas, E. 2012 Remediation of water pollution caused by pharmaceutical residues based on electrochemical separation and degradation technologies: a review. *Environment International* **40** (1), 212–229. http://dx.doi.org/10.1016/j.envint.2011.07.012.

Wang, N., Zheng, T., Zhang, G. & Wang, P. 2016 A review on Fenton-like processes for organic wastewater treatment. *Journal of Environmental Chemical Engineering* **4** (1), 762–787.

Webb, K. S. & Seneviratne, V. 1995 A mild oxidation of aromatic amines. *Tetrahedron Letters* **36** (14), 2377–2378.

Wu, Y., Prulho, R., Brigante, M., Dong, W., Hanna, K. & Mailhot, G. 2017 Activation of persulfate by Fe(III) species: implications for 4-tert-butylphenol degradation. *Journal of Hazardous Materials* **322**, 380–386. https://hal-univ-rennes1.archives-ouvertes.fr/hal-01438110/document (accessed 19 February 2018).

Yalfani, M. S., Contreras, S., Medina, F. & Sueiras, J. 2009 Phenol degradation by Fenton's process using catalytic in situ generated hydrogen peroxide. *Applied Catalysis B: Environmental* **89** (3–4), 519–526.

Yao, Y., Cai, Y., Wu, G., Wei, F., Li, X., Chen, H. & Wang, S. 2015 Sulfate radicals induced from peroxymonosulfate by cobalt manganese oxides ($Co_xMn_{3-x}O_4$) for Fenton-like reaction in water. *Journal of Hazardous Materials* **296**, 128–137.

First received 19 August 2018; accepted in revised form 19 November 2018. Available online 29 November 2018